CONDENSED-MATTER SPECTROSCOPY

Luminescence Spectroscopy of Excitons and Antisite Defects in Lu₃Al₅O₁₂ Single Crystals and Single-Crystal Films

Yu. Zorenko[a], T. Voznyak[a], V. Gorbenko[a], T. Zorenko[a], A. Voloshinovskiĭ[b], V. Vistovsky[b], M. Nikl[c], K. Nejezchleb[d], V. Kolobanov[e], and D. Spasskiĭ[e]

[a] Ivan Franko University of Lviv, Lviv, 79017 Ukraine
[b] Ivan Franko University of Lviv, Lviv, 79005 Ukraine
[c] Institute of Physics, Academy of Sciences of the Czech Republic, 16253 Prague, Czech Republic
[d] CRYTUR Ltd, 51119 Turnov, Czech Republic
[e] Moscow State University, Moscow, 119899 Russia

Received April 3, 2007

Abstract—The nature of the intrinsic luminescence of the lutetium aluminum garnet $Lu_3Al_5O_{12}$ (LuAG) has been analyzed on the basis of time-resolved spectral kinetic investigations upon excitation of two model objects, LuAG single crystals and single-crystal films, by pulsed X-ray and synchrotron radiations. Due to the differences in the mechanisms and methods of crystallization, these objects are characterized by significantly different concentrations of Lu_{Al} antisite defects. The energy structure of luminescence centers in LuAG single crystals (self-trapped excitons (STEs), excitons localized near antisite defects, and Lu_{Al} antisite defects) has been established. For single-crystal LuAG films, grown by liquid-phase epitaxy from a Pb-containing flux, the energy parameters of the following luminescence centers have been determined: STEs in regular (unperturbed by the presence of antisite defects) sites of the garnet lattice and excitons localized near Pb^{2+} ions. The structure of the luminescence centers, related to the background emission of impurity Pb^{2+} ions, has also been established in the UV and visible ranges. It is suggested that, in contrast to the two-halide hole self-trapping, a self-trapped state similar to STEs in simple oxides (Al_2O_3, Y_2O_3) is formed in LuAG; this state is formed by self-trapped holes in the form of singly charged O^- ions and electrons localized at excited levels of Lu^{3+} cations.

PACS numbers: 78.55.-m

DOI: 10.1134/S0030400X08010116

INTRODUCTION

Phosphors based on single-crystal films of complex oxides $Y_3Al_5O_{12}$ (YAG) and $Lu_3Al_5O_{12}$ (LuAG) with a garnet structure, doped with Ce^{3+} ions, and grown from flux by liquid-phase epitaxy (LPE), are characterized by much lower concentrations of substitutional defects in the form of antisite defects (ADs) of the Y_{Al} and Lu_{Al} types, in comparison with their bulk single-crystal analogs grown from melt by the Czochralski or modified Bridgman methods [1, 2]. As a result, single-crystal phosphor films contain no channels of excitation energy dissipation that are related to the above-mentioned types of defects (which compete with the luminescence of Ce^{3+} ions [3–5]). That is why single-crystal films are also a convenient model object of studying the processes of relaxation of low-energy excitations in complex oxides with several cation sublattices, in particular, luminescence of excitons [1–5].

In this context, comparative analysis of the time-resolved luminescence spectra of garnet single crystals and single-crystal films upon excitation by synchrotron radiation is an extremely informative method, because it makes it possible to localize excitation only in the bulk of single-crystal films, both near the fundamental absorption edge and in the range of interband transitions in garnets [1–5]. This circumstance allows one to investigate the intrinsic luminescence of the chosen types of garnets by the example of single-crystal, excluding the corresponding luminescence of centers related to ADs and vacancy-type defects, as this generally occurs in single crystals of the same composition [6–9]. The presence of these types of defects in oxide single crystals is related to the thermodynamic conditions of their synthesis from melt in gaseous media with a low partial oxygen pressure at much higher (1850–1950°C) growth temperatures in comparison with the synthesis of single-crystal films (950–1050°C) [10, 11].

It should be noted that the luminescence of excitons and ADs in garnets has been studied well for undoped and Ce^{3+}-doped $Y_3Al_5O_{12}$ (YAG) single-crystal films and single crystals [1, 4–8]. The $Lu_3Al_5O_{12}$ (LuAG) garnet has been investigated much less thoroughly [9]. At the same time, the results of the investigation of LuAG:Ce single crystals and single-crystal films as promising high-speed scintillators, reported by us previously [2, 3], indicate a significant difference in their

luminescence properties. These differences are primarily related to the intrinsic luminescence of garnet single crystals and single-crystal films. In turn, these results stimulated our investigations of the features of intrinsic luminescence (to which we assign the luminescence of ADs and excitons) of undoped LuAG single crystals and single-crystal films upon excitation by pulsed X-ray and synchrotron radiations in the temperature range 8–300 K. The results of these investigations are reported here.

EXPERIMENTAL

LuAG single crystals were grown at CRYTUR Ltd (Czech Republic). Growth was performed from melt by the Czochralski method in Mo crucibles in a reducing atmosphere from a charge based on Lu_2O_3 (purity 5N) and Al_2O_3 (purity 4N) oxides. These single crystals were also used to obtain substrates $7 \times 7 \times 1$ mm in size to grow single-crystal LuAG films. Substrates of another type were also used, i.e., plates of the same size cut from YAG single crystals. Single-crystal LuAG and LuAG:Ce films were grown on LuAG and YAG single-crystal substrates by LPE from a supercooled melt–solution based on the $PbO–B_2O_3$ flux. The film growth was performed at the Laboratory of Materials for Optoelectronics, Franko Lviv National University, from the same charge that was used to grow single crystals. When single-crystal LuAG and LuAG:Ce films were grown on YAG substrates, no additional doping was used to decrease the lattice mismatch between the film and substrate. The procedure of growth of single-crystal LuAG and LuAG:Ce films was described by us in detail in [12, 13].

Two types of single-crystal films were chosen for investigations: (i) 22-μm-thick single-crystal LuAG films grown on LuAG single-crystal substrates (denoted below as LuAG1) and (ii) 36-μm-thick single-crystal LuAG films grown on YAG single-crystal substrates (denoted below as LuAG2). The composition of both single-crystal films corresponded to the chemical formula $Lu_3Al_5O_{12}$. At the same time, LuAG2 films, in comparison with LuAG1, had a much higher (by a factor of ~2.5) background concentration of impurity lead ions Pb^{2+}, which are incorporated into single-crystal films during their growth from lead-containing fluxes. The relative concentrations of lead ions in LuAG2 (0.0025 at %) and LuAG1 (0.0010 at %) films were determined from the X-ray microanalysis data and the optical absorption at a wavelength of 262 nm, which corresponds to the $^1S_0 \longrightarrow {}^3P_1$ optical transition in Pb^{2+} ions [12–14].

The time-resolved luminescence and luminescence excitation spectra and the luminescence decay kinetics were investigated upon synchrotron radiation excitation on the SUPERLUMI station at HASYLAB, DESY (Hamburg, Germany). The luminescence spectra were investigated both in the integral mode and in the time intervals 1.2–6.2 ns (fast components) and 150–200 ns (slow components) after excitation with a synchrotron radiation pulse with an energy of 3.7–25 eV and a width of 0.127 ns. The excitation spectra were corrected to the spectral sensitivity of the Al lattice and the energy of the incident synchrotron radiation beam. The luminescence decay kinetics of single crystals and single-crystal films was measured upon synchrotron radiation excitation in the time interval 0–200 ns at 8 and 300 K in the integral mode of a 6358 P photomultiplier (Hamamatsu). For comparison, we also investigated the luminescence spectra of LuAG single crystals and the luminescence decay kinetics for these crystals upon excitation by an X-ray pulse (width 1.5–2 ns) in the temperature range 77–300 K.

RESULTS AND DISCUSSION

The luminescence spectra of LuAG single crystals, recorded at (a) 8 and (b) 300 K upon synchrotron radiation excitation with energies of 7.03, 7.155, and 7.41 eV in the exciton region (6.8–7.8 eV), are shown in Fig. 1 (curves *1–3*, respectively). It can be seen that the structure of the luminescence spectra of LuAG single crystals measured is similar in measurements of the integral (*2i*), slow (*2s*), and fast (*2f*) luminescence components. The luminescence spectrum of LuAG single crystals at 8 K upon synchrotron radiation excitation with an energy of 7.155 eV in the maximum of the excitation band in the exciton region (curve *2*) is a superposition of two dominant bands, peaking at 4.36 (284 nm) and 3.76 eV (329 nm), which are, respectively, due to the exciton luminescence and recombination luminescence of Lu_{Al} ADs [2–4]. It should be noted that the band at 4.36 eV in the spectra of LuAG single crystals (Fig. 1, curve *2i*) is asymmetrically broadened to higher energies; this fact indicates the presence of another weak exciton luminescence in LuAG single crystals. The position of this band at 4.95 eV (250 nm), determined from the spectra of the fast and slow luminescence components (Fig. 1a, curves *2f*, *2s*), coincides with the position of the luminescence band due to self-trapped excitons (STEs) in LuAG:Ce single crystals and single-crystal films [2, 3]. Hence, this luminescence band is due to the radiative relaxation of STEs in regular, unperturbed by the presence of defects or impurities, lattice sites in LuAG single crystals. The much lower (in comparison with the intensity of the band at 4.36 eV) intensity of the band at 4.95 eV in the luminescence spectrum of LuAG single crystals indicates that radiative relaxation of excitons in single crystals occur predominantly near Lu_{Al} ADs. Below, we will refer to the luminescence centers of such type as excitons localized near defects or impurities; in the case under consideration, excitons localized near ADs (LE(AD) centers).

The luminescence intensity both in the bands due to LE(AD) and Lu_{Al}-AD centers and in the band at 2.76 eV depends on the excitation energy in the exciton

region (Fig. 1a). The highest light yield of the luminescence of LE(AD) centers was observed upon synchrotron radiation excitation with an energy 7.16 eV (173 nm) (Fig. 1a, curve *1*), which corresponds to the formation energy of a localized exciton of such type in LuAG single crystals. In this case, the ratio of the luminescence intensities of LE(AD) and AD centers in the bands at 4.36 and 3.76 eV was 1.65. The highest luminescence intensity of Lu_{Al}-ADs is observed upon synchrotron radiation excitation with an energy of 7.03 eV (176 nm) (curve *3*), which corresponds to the position of the local Lu_{Al}-AD level in the LuAG bandgap [2, 3]. In this case, the ratio of the luminescence intensities of LE(AD) and AD centers in the corresponding bands is 1.32. The increase in the AD luminescence intensity upon synchrotron radiation excitation with an energy of 7.07 eV (onset of the fundamental absorption edge) in comparison with the spectrum measured upon excitation with an energy of 7.41 eV (maximum of STE luminescence excitation [2, 3]) leads to a red shift of the maximum of the LE(AD) luminescence band (to 4.30 eV) (Fig. 1, curves *3* and *1*, respectively).

With an increase in temperature from 8 to 300 K, luminescence quenching of LE(AD) centers in the band at 4.36 eV and increase in the luminescence intensity of Lu_{Al} ADs in the band at 3.76 eV is observed in LuAG single crystals (Fig. 1b). On the whole, this behavior is in agreement with the data of [15]. At room temperatures, the dominant band in the luminescence spectrum of LuAG single crystals is the Lu_{Al}-AD band. The luminescence bands due to LE(AD) and AD centers at 300 K peak, respectively, at 4.15 eV (298 nm) and 3.68 eV (336 nm).

At 8 K, the luminescence spectrum of LuAG single crystals also contains a wide band in the visible range, peaking at 2.76 eV (448 nm), which is obviously due, not to Lu_{Al} ADs, but to some other structural defects in LuAG single crystals (Fig. 1a). The 2.76-eV luminescence band of LuAG single crystals is most effectively excited by synchrotron radiation with an energy of 7.16 eV, which corresponds to the maximum luminescence excitation for LE(AD) centers in LuAG single crystals in the exciton region (curve *2i*). This fact indicates the existence of a certain relationship between the conditions for luminescence excitation in LE(AD) and defect centers at 2.76 eV in LuAG single crystals. At the same time, the 2.76-eV luminescence band, which is clearly observed at 8 K (Fig. 1a, curves *1–3*), is unresolved in the spectra of LuAG single crystals at 300 K (Fig. 1b). Nevertheless, the differences in the shape of the luminescence band due to Lu_{Al} ADs in the long-wavelength region, measured at 300 K upon synchrotron radiation excitation with energies of 7.07 (175 nm) and 6.92 eV (179 nm) (Fig. 1, curves *1i* and *2i*, respectively), allow one to select a band at 2.76 eV in the difference luminescence spectrum (Fig. 1b, curve *3*).

It should be noted that YAG single crystals, isostructural to LuAG, exhibit luminescence of F^+ (400 nm)
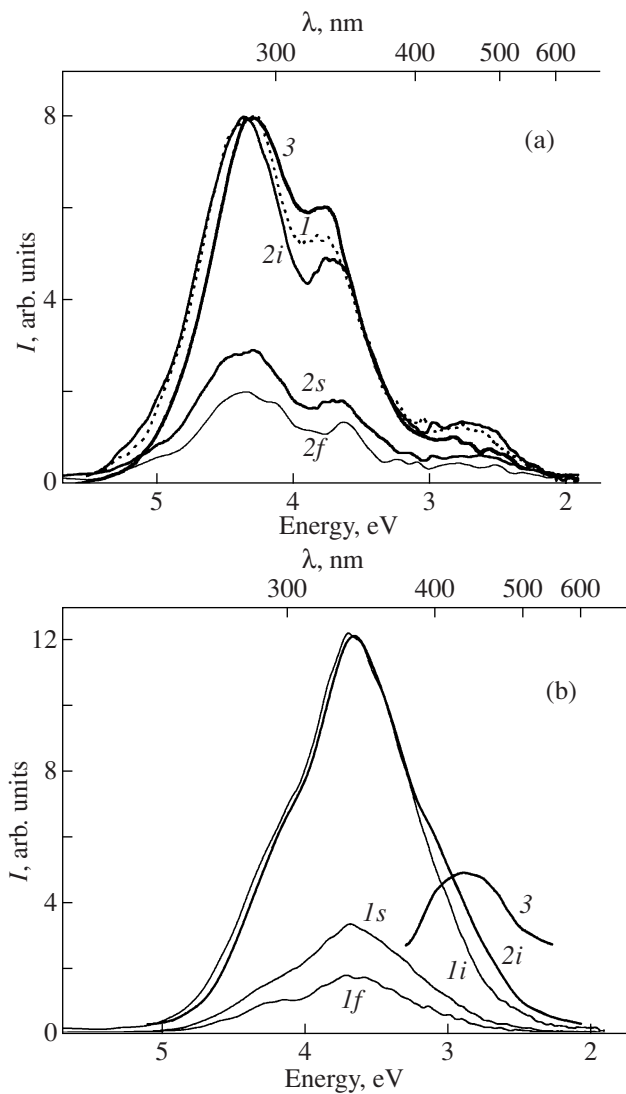
Fig. 1. Luminescence spectra of LuAG single crystals at (a) 8 and (b) 300 K for detection of the (*i*) integral, (*f*) fast, and (*s*) slow components upon synchrotron radiation excitation with an energy of 7.41–7.42 eV near the fundamental absorption edge of this garnet. Clarifications in the text.

[16] and F (460 nm) centers in the range 350–500 nm [17]. The corresponding luminescence excitation peaks for these centers are at 3.44, 5.16 (F^+), and 6.2 (F) eV [13, 14]. Therefore, by analogy with the luminescence of YAG single crystals [16, 17] the 2.76-eV luminescence band of LuAG single crystals can be assigned to the luminescence of F centers. This suggestion is confirmed by the proximity of the luminescence band of F centers in YAG (2.76 eV) and the band at 2.7 eV in LuAG single crystals, as well as by the absence of this band in the luminescence spectra of single-crystal LuAG films (Fig. 2), which are characterized by an extremely low concentration of vacancy-type defects [1–5]. Since the intensity in the band at 2.76 eV is maximum upon luminescence excitation in the exciton
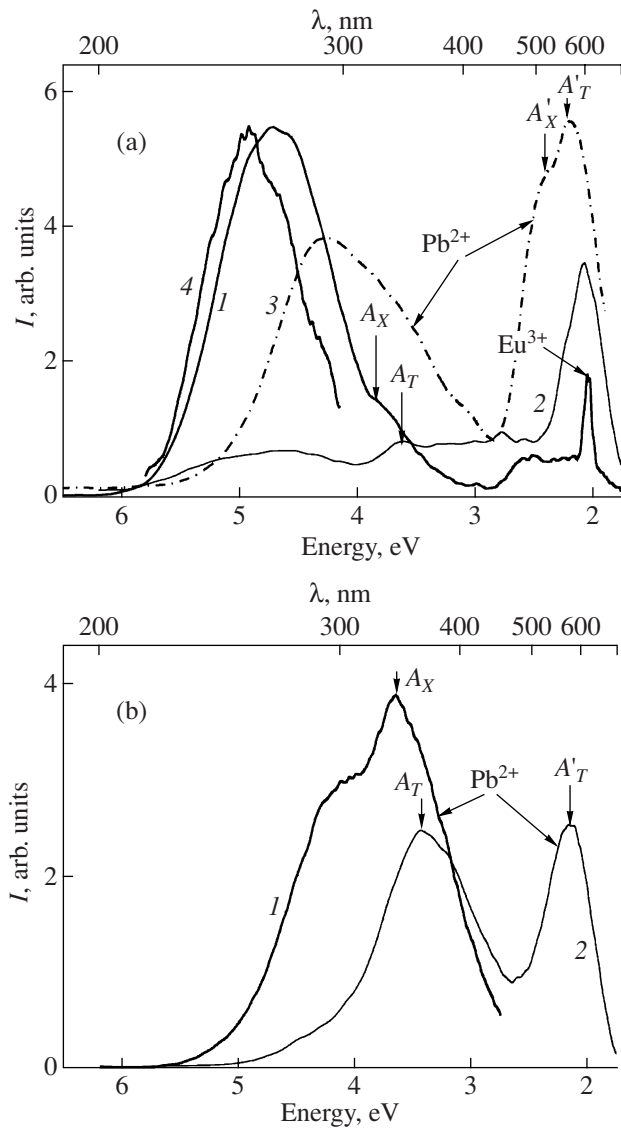
Fig. 2. Luminescence spectra of (*1*, *2*) LuAG1, (*3*) LuAG2, and (*4*) LuAG:Ce single-crystal films at (a) 8 and (b) 300 K upon synchrotron radiation excitation with energies of (b, *1*) 6.98, (a, *2*; a, *3*) 7.155, and (a, *4*) 7.4 eV in the exciton region and with an energy of 11.25 eV in the region of interband transitions in LuAG (a, *2*; b, *2*).

region, we can suggest that the luminescence of *F* centers in LuAG single crystals is most effectively excited under radiative decay of excitons localized near these centers.

Thus, the intrinsic emission of LuAG single crystals at 8 and 300 K is a superposition of the STE luminescence (the band peaking at 4.95 eV), dominant luminescence of localized excitons, stabilized near Lu_{Al}^{3+} ADs (LE(AD) centers) (the band at 4.36 eV), the recombination luminescence of Lu_{Al}^{3+} ADs (the band at 3.76 eV), and the luminescence of *F* centers (the band at 2.76 eV). The spectral intensity distribution for these

bands in the luminescence spectra of LuAG single crystals depends on the temperature of the experiment.

The luminescence spectra of LuAG-based single-crystal films are shown in Fig. 2 for temperatures of (a) 8 and (b) 300 K. A characteristic feature of the luminescence spectra of single-crystal LuAG films (Fig. 2), differing them from the spectra of single crystals (Fig. 1), is a much lower intensity of the intrinsic luminescence at both 8 and 300 K upon excitation in the region of interband transitions and in the exciton region. In particular, an important feature of the luminescence spectra of the LuAG1 (curves *1*, *2*) and LuAG2 (curve *3*) films, as well as the single-crystal LuAG:Ce films (curve *4*), in comparison with the spectra of LuAG single crystals, is the absence of the AD-luminescence band peaking at 3.76 eV, both at 8 and 300 K. This feature indicates the absence of ADs in single-crystal films. In comparison with the spectra of LuAG single crystals (Fig. 1a), the luminescence spectrum of LuAG1 films at 8 K is significantly shifted to higher energies (Fig. 2, curve *1*). In particular, upon excitation of LuAG1 films by synchrotron radiation with an energy of 7.155 eV, with the maximum of the excitation spectrum in the exciton region, the luminescence spectrum is a dominant multicomponent band peaking at 4.715 eV (262.5 nm). It should be noted that this band is shifted by 0.235 eV to lower energies with respect to the maximum of the 4.95-eV luminescence band in single-crystal LuAG:Ce films (Fig. 2a, curve *4*), which is due to the STEs in regular lattice sites of this garnet [2, 3]. The luminescence spectrum of LuAG2 films (with a higher concentration of Pb^{2+} ions in comparison with LuAG1 films) upon synchrotron radiation excitation with an energy of 7.156 eV is a dominant band peaking at 4.3 eV, which is asymmetrically broadened to higher energies due to the presence of a weak STE luminescence band peaking at 4.95 eV (Fig. 2a, curve *3*). With due regard to the spectral features of the luminescence of LuAG2 films, we can suggest that the luminescence spectrum of LuAG1 films is a superposition of two bands, peaking at 4.95 and 4.3 eV. These luminescence bands are due to, respectively, STEs in regular, unperturbed by the presence of ADs, garnet lattice sites and localized excitons whose radiative relaxation occurs near Pb^{2+} ions (LE(Pb) centers), which are the main background impurity in single-crystal films. The latter suggestion is confirmed by the strong dependence of the peak positions and intensities of the luminescence bands of localized excitons in LuAG1 and LuAG2 films on the concentration of Pb^{2+} ions (Fig. 2a, curves *1*–*3*) and their significant difference from the STE luminescence characteristics of single-crystal LuAG:Ce films (curve *4*).

In the lower energy range (>4 eV), the luminescence spectra of LuAG1 and LuAG2 films exhibit the characteristic two-component structure of the luminescence spectrum of the background impurity—Pb^{2+} ions (Figs. 2a, 2b). At 8 K, this structure contains an unre-

solved luminescence band in the UV range (4.0–3.0 eV), peaking at 3.85 eV, which is overlapped to a large extent with the luminescence band of LE(Pb) centers, and a complex luminescence band in the visible range (2.8–1.8 eV) with maxima at 2.21 and 2.40 eV. The existence of two luminescence bands of comparable intensity in the UV and visible ranges upon excitation in the exciton region (Fig. 2a, curve *2*) and the region of interband transitions (Fig. 2b, curve *3*) is due to their different nature and different mechanisms of excitation of luminescence of Pb^{2+} ions in single-crystal LuAG films [18, 19]. The UV emission band of single-crystal LuAG films is due to the radiative transitions from relaxed electronic states of single Pb^{2+} ions or their aggregates with Pt^{4+} ions [18, 19], whereas the band in the visible range is due to pair or cluster centers formed by Pb^{2+} ions [18]. The preferred mechanism of excitation of such pair/cluster centers is charge-transfer transitions ($Pb^{2+} \longrightarrow Pb^{3+} + e$) with formation of localized excitons near these pair centers (see also [20, 21]). It should be noted that the doublet structure of the luminescence bands of Pb^{2+} ions in the visible and UV ranges (respectively, A_T and A_X components and A_T' and A_X' components, Figs. 2a and 2b) can be due to the radiative transitions from the *T* and *X* minima of the $^3P_1$ and $^3P_0$ excited states of the Pb^{2+} ion with the ns^2 electronic configuration, characterized by Jahn–Teller splitting [22]. The strong narrow luminescence band at 2.04 eV in the emission spectrum of the LuAG film (Fig. 2a, curve *1*) is likely to be due to background impurity Eu^{3+} ions.

Upon synchrotron radiation excitation with an energy of 11.25 eV in the region of interband transitions in LuAG ($E_g = 8.13$ eV [2, 3]), the emission of the Pb^{2+} ions in the visible range is dominant in the luminescence spectrum of LuAG films (A_X' component at 2.09 eV) (Fig. 2, curve *2*). The wide plateau in the range 3.7–2.5 eV is likely to be due to the superposition of the A_X component of the UV luminescence band of Pb^{2+} ions (peaking at 3.63 eV) and the unresolved A_T' component of pair Pb^{2+}-containing centers of comparable intensity. The luminescence of excitons in LuAG1 films upon excitation with an energy of 11.25 eV in the region of interband transitions is observed in a weak complex band peaking at 4.65 eV, which is obviously a superposition of the luminescence of STE and LE(Pb) centers (Fig. 2a, curve *2*). Note that the intensity of excitation of the STE luminescence in the region of interband transitions (Fig. 2a, curve *2*) is much lower than that in the exciton region (Fig. 2a, curves *1*, *4*).

The luminescence spectrum of LuAG1 films significantly changes in the room-temperature range (Fig. 2b). Upon excitation with an energy of 6.97 eV, with the maximum of the excitation band in the exciton region, the A_T luminescence component of Pb^{2+} ions,

peaking at 3.65 eV, is dominant in the UV luminescence spectrum of LuAG1 films. Along with this band, a band at 4.13 eV, which is due to the luminescence of LE(Pb) centers, is also observed. Upon excitation of LuAG1 films by synchrotron radiation with an energy 11.25 eV in the region of interband transitions, at 9 and 300 K, luminescence of Pb^{2+} ions in the bands at 3.42 and 2.16 eV (A_X and A_X' component) is dominant, whereas the luminescence of LE(Pb) centers is almost quenched (Fig. 2b, curve *2*). The difference in the positions of the maxima in the UV luminescence band of Pb^{2+} ions in single-crystal LuAG films upon synchrotron radiation excitation in the exciton region (3.65 eV) and in the region of interband transitions (3.42 eV) is obviously due to the dominance of the A_X or A_T luminescence components of Pb^{2+} ions in the corresponding spectra and the overlap of the luminescence bands of LE(Pb) and Pb^{2+} centers (Fig. 2b, curves *1* and *2*, respectively).

Thus, the intrinsic luminescence of single-crystal LuAG films is due to the luminescence of STEs in regular, unperturbed garnet lattice sites in the band at 4.95 eV and the luminescence of excitons localized near Pb^{2+} ions (LE(Pb)) in the band at 4.3 eV. In the longer wavelength spectral region, the luminescence of single-crystal LuAG films in the bands peaking in the ranges 3.85–3.62 and 2.40–2.21 eV is due to the presence of the background impurity Pb^{2+} ions. A characteristic feature of the luminescence of single-crystal LuAG films is the much lower (by almost by an order of magnitude) luminescence intensity of LE(Pb) and Pb^{2+} centers in comparison with the luminescence intensity of LE(AD) and Lu_{Al}-AD centers in LuAG single crystals upon excitation in the exciton region (Fig. 1, curve *1*) and in the region of interband transitions (Fig. 2, curve *2*).

The temperature dependence of the luminescence spectra of LuAG single crystals in the range 77–290 K upon X-ray pulsed ($\Delta\tau = 1.5$ ns) excitation is shown in more detail in Fig. 3a. The temperature dependences of the luminescence intensity of STE, LE(AD), and Lu_{Al}-AD centers, measured, respectively, in the bands at 4.95, 4.36, and 3.76 eV, are shown in Fig. 3b (curves *1–3*, respectively). Beginning with a temperature of 77 K (actually, with 8 K, if we take into account the results shown in Fig. 1a), the STE luminescence in the band at 4.95 eV undergoes temperature quenching, and, at temperatures above 200 K, this band is almost absent in the luminescence spectra of LuAG single crystals. The thermal quenching of the STE luminescence is accompanied by some increase in the luminescence intensity of LE(AD) centers in the temperature range 8–125 K. At higher temperatures, the luminescence of LE(AD) centers undergoes temperature quenching, and its intensity at 300 K is only ~30% of the maximum luminescence intensity at 125 K. In turn, the thermal quenching of the luminescence of STE and LE(AD)
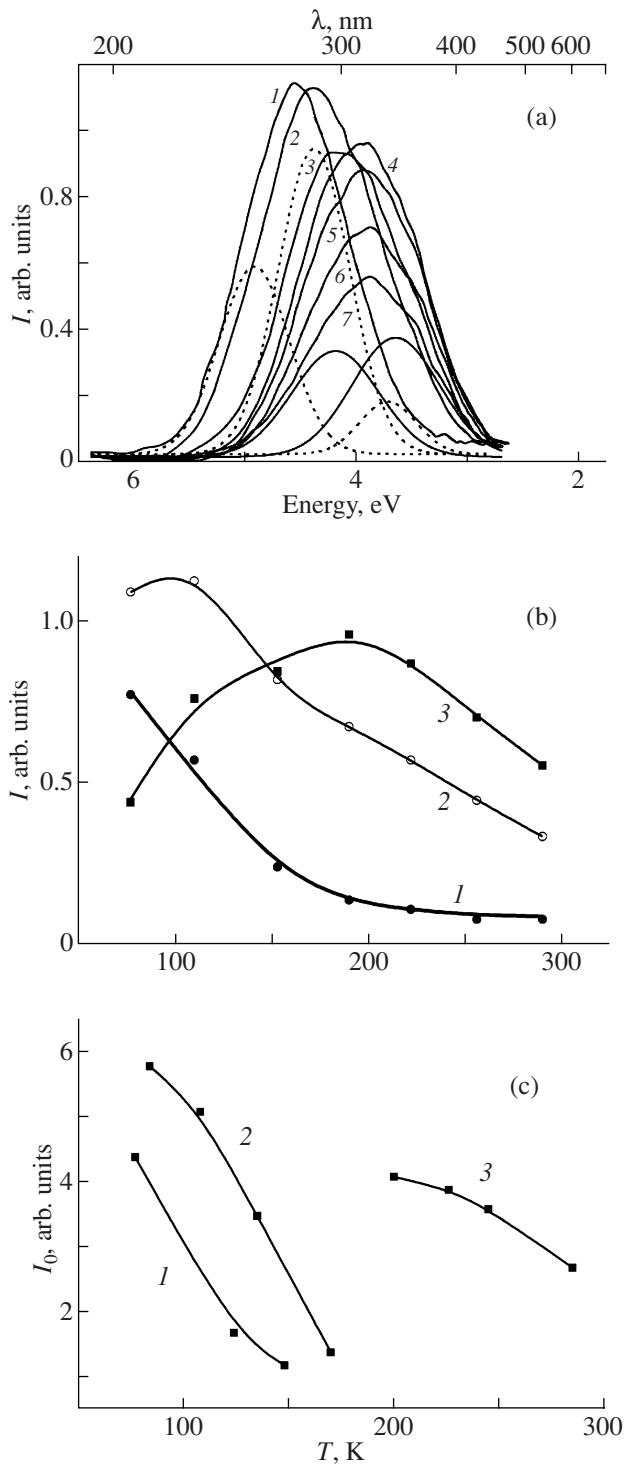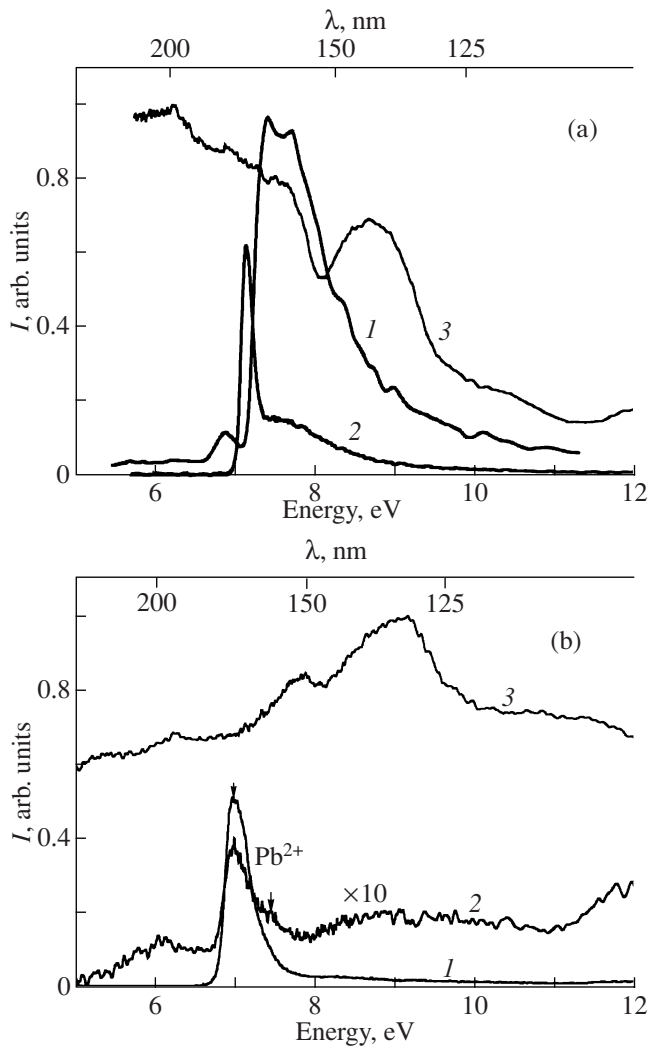
Fig. 3. (a) Luminescence spectra of LuAG single crystals upon pulsed X-ray excitation in the temperature range 77–290 K: T = (*1*) 77, (*2*) 110, (*3*) 153, (*4*) 190, (*5*) 222, (*6*) 256, and (*7*) 290 K (the luminescence spectra at 77 and 300 K are decomposed in elementary components); (b) the temperature dependences of the luminescence intensities of STE, LE(AD), and Lu$_{Al}$-AD centers in the bands peaking, respectively, at (*1*) 4.95, (*2*) 4.36, and (*3*) 3.76 eV; (c) the temperature dependences of the intensities of superslow luminescence components of these centers, determined from the initial portions of the decay curves.

centers is accompanied by the enhancement of the AD luminescence in the band peaking at 3.76 eV (curve *3*). The maximum luminescence intensity in this band is obtained at a temperature of 190 K, above which the luminescence of these centers undergoes thermal quenching. At 300 K, the intensity of the Lu$_{Al}$-AD luminescence is ~0.5 of the maximum luminescence intensity at 190 K.

To explain the observed temperature dependences of the different components of the complex intrinsic luminescence band of LuAG single crystals, we suggest that the electrons or holes that are released after decay of STEs in regular lattice sites, beginning with 8 K, migrate to deeper (LE(AD)) centers, and, after their thermal decay at 120 K, to Lu$_{Al}$ ADs. In turn, they are released from the latter at temperatures ≥190 K. Thus, the temperature dependences of the shape of the luminescence spectra and the luminescence intensity in the UV range for LuAG single crystals (Figs. 3a, 3b) reflect successive processes of thermal delocalization, transfer, and subsequent localization of charge carriers from shallower to deeper centers in the STE ⟶ LE(AD) ⟶ Lu$_{Al}$ AD sequence with the corresponding luminescence bands peaking at 4.95, 4.36, and 3.76 eV (250, 284, and 329 nm).

The structure of the luminescence excitation spectrum of STEs in LuAG is most pronounced in Fig. 4a, where the excitation spectra of the integral component of the luminescence of single-crystal LuAG:Ce films at a wavelength of 250 nm (4.95 eV) and the luminescence of LuAG1 films at a wavelength of 260 nm (4.76 eV) are shown (curves *1* and *2*, respectively). Note a significant difference in the shape of the exciton luminescence excitation spectra for these two types of single-crystal films. In particular, the STE luminescence excitation spectrum in the band at 4.95 eV in single-crystal LuAG:Ce films (curve *1*) contains a weak band at 6.88 eV and a characteristic doublet structure, consisting of two wide bands of comparable intensity, at 7.4 and 7.71 eV, which are due to the presence of two radiative STE levels [2, 3]. The presence of these two excited STE levels can be responsible for the existence of two radiative transitions with significantly different luminescence decay times.
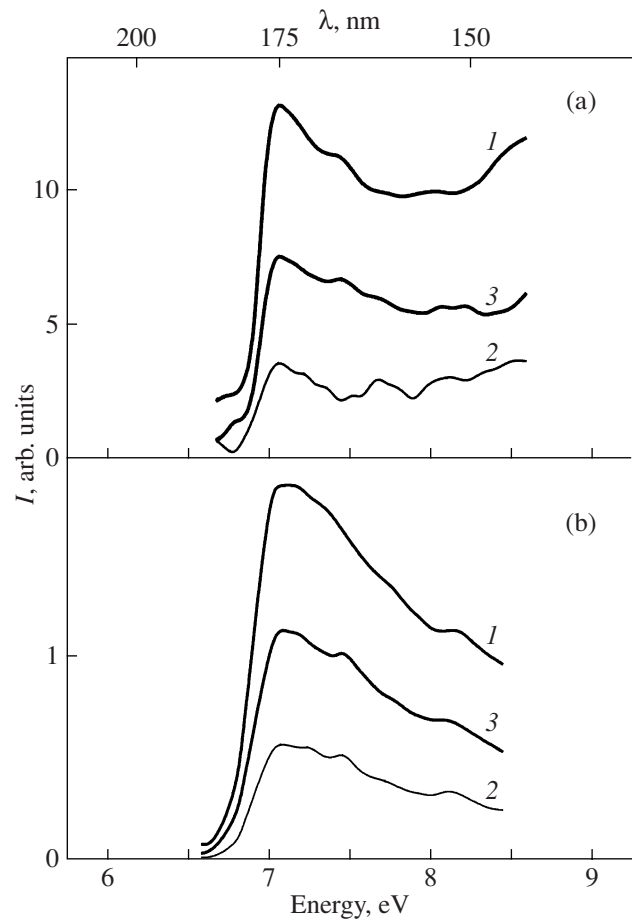
The luminescence excitation spectra of LuAG single crystals at a wavelength of 260 nm (4.76 eV) upon synchrotron radiation excitation near the fundamental absorption edge of this garnet (6.6–8.5 eV) at (a) 8 and (b) 300 K are shown in Fig. 5. With due regard to the temperature dependence of the spectral components of the luminescence of LuAG single crystals (Figs. 1, 3), the excitation spectrum at a wavelength of 260 nm at 8 K will be determined to a larger extent by the luminescence of LE(AD) centers in the band at 4.36 eV and a partial contribution of the STE luminescence in the band at 4.95 eV, whereas the excitation spectrum at the same the wavelength at 300 K will be predominantly

Fig. 4. (a) Luminescence excitation spectra of STE and LE(Pb) centers, measured at 8 K at wavelengths of 250 nm for single-crystal LuAG:Ce films (a, *1*) and 260 nm for LuAG1 films (a, *2*), and (b) the luminescence excitation spectrum of Pb^{2+} ions in LuAG1 films in the UV and visible spectral ranges, measured at room temperature at wavelengths of (*1*) 350 and (*2*) 580 nm. For comparison, the reflection spectra of single-crystal LuAG films (curves *3*) at (a) 8 and (b) 300 K are shown.
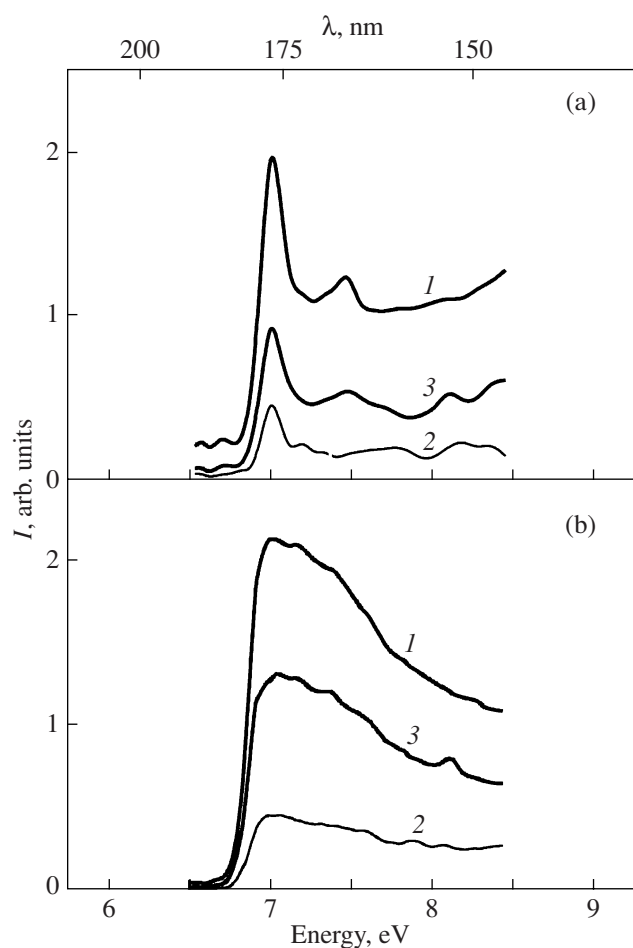

Fig. 5. Luminescence excitation spectra of STE and LE(AD) centers in LuAG single crystals, measured at wavelengths of 260 nm, at (a) 8 and (b) 300 K, in the cases of detection of the (*1*) integral, (*2*) fast, and (*3*) slow components.

controlled by the luminescence of LE(AD) centers (Fig. 5b).

It can be seen in Fig. 5a that the luminescence of LE(AD) centers in LuAG single crystals is excited at 8 K in a wide doublet band with maxima at 7.05 and 7.45 eV. Detection of the integral (curve *1*) and slow (curve *3*) luminescence components reveals an additional band peaking at 8.13 eV on the high-energy wing of the doublet band, which, apparently, corresponds to the onset of interband transitions in LuAG [2, 3]. Thus, the excited state of an LE(AD) center in LuAG single crystals is characterized by the existence of at least two levels with significantly different radiative transition

probabilities. This feature is evidenced by a certain difference in the luminescence excitation spectra of LE(AD) centers in the cases of detection of the fast (curve *2*) and slow (curve *3*) components. In particular, the band at 7.45 eV, which is almost absent in the excitation spectrum of the fast (curve *2*) luminescence component, is nevertheless pronounced in the spectra of the integral (curve *1*) and slow (curve *3*) luminescence components (Fig. 5a, curves *1* and *2*, respectively).

The additional bands at 7.22 and 7.67 eV in the excitation spectrum of the fast luminescence component recorded at 8 K (curve *2*) are likely to correspond to the luminescence excitation bands of STEs in LuAG single crystals, since their spectral position is fairly close to the position of the similar luminescence excitation bands (7.28 and 7.68 eV) of STEs in LuAG:Ce single crystals [2, 3].

The pronounced doublet structure of the excitation spectrum for both the integral and slow luminescence components of STEs in single-crystal LuAG films and LE(AD) centers in LuAG single crystals indicates the

Fig. 6. Luminescence excitation spectra of Lu_{Al} ADs in LuAG single crystals, measured at a wavelength of 330 nm, at (a) 8 and (b) 300 K, in the cases of detection of the (*1*) integral, (*2*) fast, and (*3*) slow components.

formation of excitons characterized by the presence of two excited levels with significantly different radiative transition probabilities (presumably, transitions of the singlet–singlet (σ) and triplet–singlet (π) types) [23]. Within this suggestion, the excitation bands at 7.4 and 7.05 eV may belong to the σ components of the STE and LE(AD) luminescence with a small (several nanoseconds) decay time constant, whereas the excitation bands at 7.71 and 7.45 eV may correspond to the dominant π component of the LE(AD) luminescence with intermediate (several tens or hundreds of nanoseconds) and slow (several microseconds or even milliseconds) decay time constants. In the latter case, one can suggest the existence of two neighboring radiative levels, among which the lower level is metastable with respect to the upper one. A similar structure of the excitation spectrum is observed for the STE luminescence in other oxide compounds, in particular, Al_2O_3 [24, 25].

Similar considerations can be used to analyze the luminescence excitation spectrum of Lu_{Al} ADs at 8 and 300 K (Figs. 6a and 6b, respectively). A well-resolved

doublet structure of two bands with a characteristic strong narrow peak at 7.01 eV and a weaker peak at 7.46 eV in the exciton region indicates the formation of a bound exciton with two radiative levels characterized by different dipole moments, which is responsible for the existence of the fast and slow luminescence components. The maximum excitation of the fast components corresponds to 7.01 eV (Fig. 6a, curve *2*), whereas the slow components of the Lu_{Al}-AD luminescence are also excited in the band at 7.47 eV (curve *3*). Thus, a bound exciton is formed, which is localized directly at an Lu_{Al} AD with an electronic structure different from that of STE and LE(AD) centers. With an increase in temperature to 300 K, the highest maximum of excitation of the Lu_{Al}-AD luminescence (upon measurement of the integral luminescence component) undergoes a temperature shift up to 6.99 eV. In this case, the difference in the positions of the maxima upon measurement of the fast (6.98 eV) and slow (7.03 eV) luminescence components can clearly be seen. This phenomenon is typical of the bound exciton luminescence in different oxide compounds [2, 3, 23–26]. In particular, a similar spectral structure was observed by us previously [2, 3] in the luminescence excitation spectra of bound excitons localized near Ce^{3+} ions in LuAG single crystals and single-crystal films. This difference in the excitation spectra for the fast and slow components (Fig. 6b) may indicate the formation of singlet and triplet states of bound excitons localized directly at impurities and defects in compounds with a garnet structure.
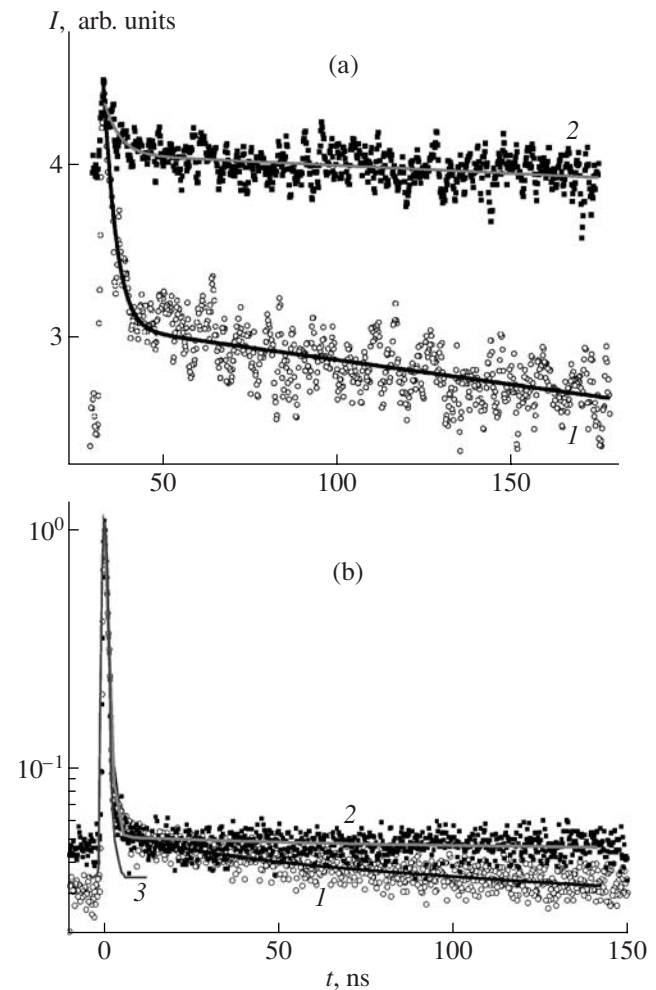
The luminescence excitation spectrum of LuAG1 films (Fig. 4a, curve *2*) at a wavelength of 260 nm at 8 K, which is most adequate to the luminescence excitation spectrum of LE(Pb) centers, has a typical two-band structure with maxima at 7.14 and 7.50 eV. The shape of this excitation spectrum (a strong narrow band in the exciton absorption region) indicates the formation of an exciton localized near a defect or impurity.

It should be noted that the position of the luminescence excitation band of LE(Pb) centers (Fig. 4a, curve *2*) significantly differs from that in the luminescence excitation spectra of Pb^{2+} ions (Fig. 4b) in the UV and visible spectral ranges, measured respectively at wavelengths of 350 and 580 nm (curves *1, 2*). Luminescence of Pb^{2+} ions in the UV range is excited in the dominant band at 6.97 eV in the exciton region, whereas in the visible range, it is excited in bands at 6.97 and 6.10 eV. The temperature shift of the LuAG bandgap in the range 8–300 K, which was estimated by us from the shift of the dominant minimum in the reflection spectrum of single-crystal LuAG films in the exciton region (Figs. 4a, 4b, curves *3*) to be 0.085 eV, is much smaller than the difference in the positions of the luminescence excitation maxima for LE(Pb) and Pb^{2+} centers (0.19 eV). Hence, one can state that the excitation band peaking at 6.97 eV at 300 K corresponds to the energy of formation of a bound exciton localized at a Pb^{2+} ion (similar to bound excitons localized at Lu_{Al} ADs in

LuAG single crystals or Ce^{3+} ions in single-crystal LuAG:Ce films [2, 3]). The band peaking at 6.10 eV in the luminescence excitation spectrum of LuAG1 films is due to the charge-transfer transitions between Pb^{2+} ions and the bottom of the conduction band [14, 18].

The above considerations with respect to the energy structure of STE, LE(AD), and Lu_{Al}-AD centers are confirmed by the data on the luminescence decay kinetics for LuAG single crystals at 8 K upon synchrotron radiation excitation with an energy of 7.97 eV in the maximum of LE(AD) luminescence excitation in the exciton region (Fig. 7a). The decay curves were approximated by the sum of three exponential components: $I(t) = I_0 + \sum_i^3 A_i \exp(-t/\tau_i)$. It can be seen in Fig. 7a that the luminescence decay curve for LE(AD) centers, measured in the integral mode (curve *1*), contains a very fast ($\tau_1 = 2.1$ ns, 42.1% of the initial luminescence intensity) and two slower (with 16.9 ns (29.9%) and 734 ns (28.0%)) components, which may correspond, respectively, to the σ and π luminescence components of LE(AD) centers. This suggestion is confirmed by the luminescence decay kinetics of LuAG single crystals at 300 K (Fig. 6a, curve *2*) upon synchrotron radiation excitation with an energy of 7.0 eV in the maximum of Lu_{Al}-AD luminescence excitation in the band at 3.68 eV (Fig. 1b). The Lu_{Al}-AD luminescence decay curve shown in this figure can also be approximated by a set of three components with $\tau_1 = 2.45$ ns (4.3%), $\tau_2 = 8.0$ ns (5.7%), and $\tau_3 = 4370$ ns (90%). As in the case with analysis of the LE(AD) luminescence decay kinetics, the use of synchrotron radiation makes it possible to select the very fast luminescence component with $\tau_1 = 2.45$ ns, which may correspond to the σ component, whereas the components with $\tau_2 = 8.0$ ns and $\tau_3 = 4370$ ns may correspond to the π component of the Lu_{Al}-AD luminescence. At the same time, due to the high repetition frequency of synchrotron radiation pulses and a narrow (200 ns) time interval for measuring the luminescence decay kinetics, detailed analysis and determination of the parameters of the luminescence π components for LE(AD) and Lu_{Al}-AD centers cannot be performed in micro- and millisecond ranges.

In this context, study of the luminescence decay kinetics of LuAG single crystals was continued upon excitation by pulsed ($\Delta t = 1.5$–2.0 ns) X rays in the temperature range 77–300 K (Fig. 8). Due to the close location of the luminescence bands of STE, LE(AD), and AD centers, the decay kinetics in the integral mode contains a set of components belonging to these three types of luminescence centers. At the same time, taking into account the temperature dependence of the intensity and shape of the UV luminescence spectrum of LuAG single crystals (Figs. 3a, 3b), one can reliably separate the components from different luminescence centers (Fig. 7). It should be noted that the temperature dependences of the decay kinetics for LuAG single

Fig. 7. (a) Luminescence decay kinetics of LuAG single crystals, measured in the integral mode upon synchrotron radiation excitation with an energy of 7.07 eV in the exciton region at (*1*) 8 and (*2*) 300 K, and (b) the luminescence decay kinetics of LuAG1 films in the (*1*) UV and (*2*) visible spectral ranges at 300 K, in comparison with the response of the recording system to a unit synchrotron radiation pulse. Clarifications in the text.

crystals, which were measured at wavelengths of 250, 280, and 320 nm (Figs. 8a–8c, respectively), are in good agreement with the temperature dependences of the shape of the luminescence spectra of STE, LE(AD), and Lu_{Al}-AD centers in LuAG single crystals in the range 77–295 K (Fig. 3b).

The data in Fig. 8a and Table 1 indicate that the luminescence decay curves for LuAG single crystals at a wavelength of 250 nm (4.95 eV) in the temperature range 77–108 K, where STE luminescence is dominant in the emission spectrum (Fig. 3b), can be approximated by a superposition of three exponentials with decay time constants lying, respectively, in the ranges of several tens of nanoseconds, several hundred nanoseconds, and several microseconds (or even milliseconds). This fact indicates that the relaxed electronic
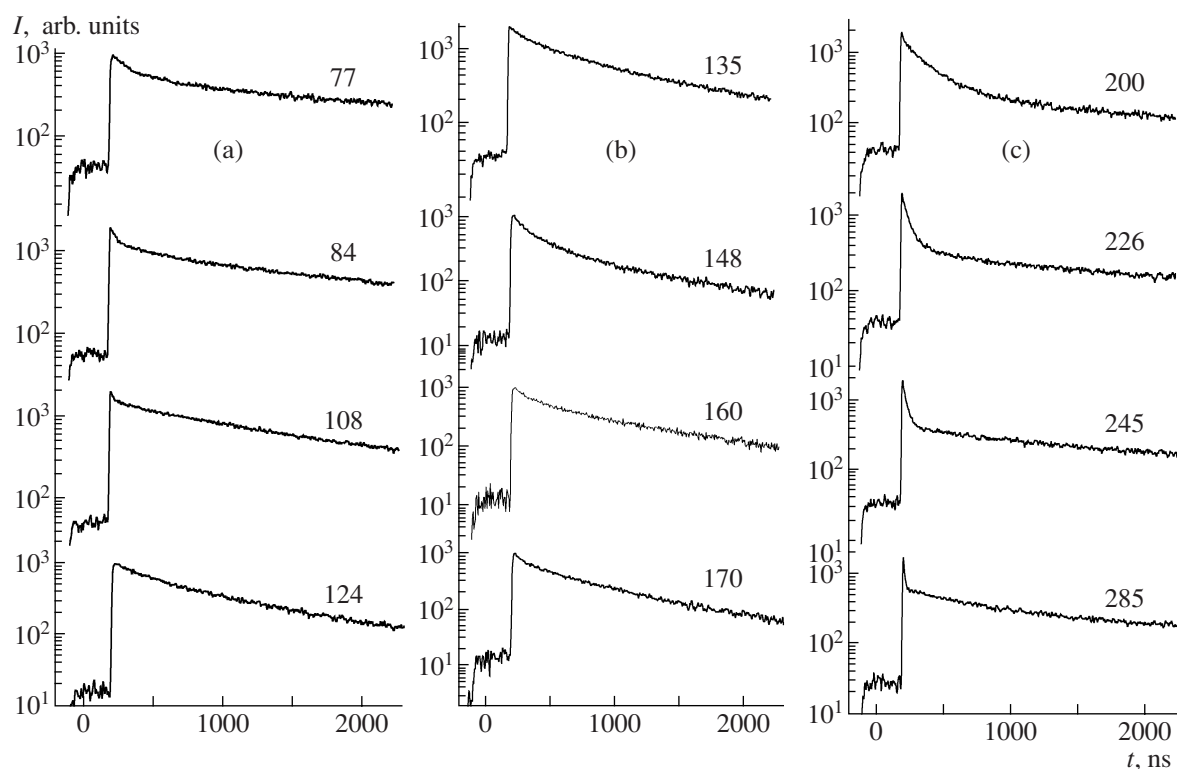
Fig. 8. Luminescence decay kinetics of single-crystal LuAG films at wavelengths of 250, 280 and 325 nm, corresponding to the maxima of the corresponding luminescence bands of (a) STE, (b) LE(AD), and (c) Lu_{Al}-AD centers in the temperature range 77–285 K. The numbers at the curves indicate temperatures.

STE state can be considered as a triplet state, from which allowed, partially allowed, and forbidden transitions may occur. Such decay kinetics is characteristic of the STE luminescence in simple oxides, in particular, Al_2O_3 [23, 24]. The temperature dependences of the decay time constants for the fast (τ_1), intermediate (τ_2), and slow (τ_3) components of the STE luminescence in LuAG single crystals in the temperature range 77–290 K are listed in Table 1.

It can be seen in Figs. 8a–8c that the character of the decay kinetics of LuAG single crystals significantly changes beginning with temperatures of 124 and 200–205 K. At these temperatures, the highest LE(AD) and AD luminescence intensity is observed (Fig. 3b, curves 2, 3). With due regard to this fact, the luminescence decay kinetics of LuAG single crystals, measured at wavelengths of 280 and 320 nm in the temperature ranges 124–170 K (Fig. 8b) and 200–285 K (Fig. 8c), is related to the greatest extent to the luminescence of LE(AD) and AD centers, respectively. Approximation of the corresponding decay curves (Table 1) indicates that the luminescence kinetics of LE(AD) and Lu_{Al}-AD centers in LuAG single crystals is qualitatively similar to the STE decay kinetics and is described by a set of three exponentials with different decay constants. This fact indicates that the excited state of these centers is also a triplet relaxed state.

It is noteworthy that the luminescence decay kinetics for Lu_{Al} ADs significantly differs from that for STE and LE(AD) centers (Fig. 8c). In particular, the decay curve for Lu_{Al} ADs at 285 K is characterized by the presence of much faster (in comparison with the luminescence of STE and LE(AD) centers) component with $\tau_1 = 7.44$ ns and dominant intermediate and slow components with $\tau_2 = 440$ ns and $\tau_3 = 3.0$ μs, respectively (Table 1). Obviously, such luminescence decay kinetics is typical of the emission of bound excitons localized directly at ADs and isoelectronic defects in oxide compounds of different structure types [27, 28]. These excitons are formed through preliminary localization of electrons or holes by non-Coulomb potential of ADs or isoelectronic defects with subsequent localization of charge carriers of opposite sign by the Coulomb potential of a localized electron or hole [27, 28].

It should be noted that, for the triplet relaxed state of STE, LE(AD), and Lu_{Al}-AD centers, the lower excited states are apparently metastable. This conclusion is evidenced by the presence of "superslow" components in the emission of these centers in the millisecond range at low temperatures, which cannot be experimentally resolved on the equipment used by us. At the same time, the existence of such components can be seen well from the presence of temperature-dependent amplitudes of the backgrounds in the initial portions of

Table 1. Decay time constants τ_1, τ_2, and τ_3 of the luminescence components of STE, LE(AD), and Lu_{Al} AD centers, derived by the standard procedure of three-component approximation $I(t) = I_0 + \sum_i^3 A_i \exp(-t/\tau_i)$ of the luminescence decay curves for LuAG single crystals at wavelengths of 250, 280, and 325 nm, respectively, in the temperature ranges 77–124, 135–170, and 200–290 K, where the emission of these centers is dominant

Type of the luminescence center and position of the maximum of the corresponding luminescence band	Temperature, K	τ_1, ns	τ_2, ns	τ_3, ns
STE, 4.905 eV	77	94.9	586.9	4238.8
	84	37.9	313.3	2284.6
	108	19.2	347.3	1667.2
	124	10.5	304.6	1281.0
LE(AD), 4.36 eV	135	74.2	385.8	1389.6
	148	55.0	252.6	1289.8
	160	43.2	231.2	1172.3
	170	47.1	333.7	937.7
AD, 3.76 eV	200	85.4	229.9	2716.3
	226	43.6	230.5	3125.4
	245	28.2	487.3	3269.6
	285	7.44	439.7	3005.1

Table 2. Spectral kinetic characteristics of the luminescence of different types of centers in LuAG single crystals and single-crystal films

Type of the luminescence center	Single-crystal LuAG films			LuAG single crystals		
	luminescence bands, eV	luminescence excitation bands, eV	decay kinetics, ns	luminescence bands, eV	luminescence excitation bands, eV	decay kinetics, ns
STE	4.95 (8 K)	7.4; 7.71 (8 K)	–	4.95 (8 K)	7.22, 7.68 (8 K)	95, 587, 4240, >10^6 (77 K)
LE(AD)	–	–	–	4.36 (8 K) 4.15 (300 K)	7.06, 7.45 (8 K)	3.1, 1100 (8 K) 74, 386, 1390, >10^6 (135 K)
LE(Pb)	4.3 (8 K), 4.13 (300 K)	7.14, 7.35 (8 K)	–	–	–	–
Lu_{Al} AD	–	–	–	3.76 (8 K) 3.68 (300 K)	7.01, 7.46 (8 K) 6.99, 7.38 (300 K)	2.45, 8.0, 4370 (8 K) 74, 386, 1390, >10^6 (300 K)
Pb^{2+}	3.85, 3.65 (8 K), 2.40, 2.26 (8 K), 3.65, 3.42 (300 K) 2.16 (300 K)	6.97 (300 K) 6.97, 6.1 (300 K)	25.6, 420 (300 K) 80.7, 9000 (300 K)	–	–	–

the decay curves, which precede the portions of intensity increase. The temperature dependences of the intensities of such initial portions for the decay curves measured at wavelengths of 250, 280, and 320 nm are shown in Fig. 3c (curves *1–3*, respectively). It can be seen in Fig. 3 that there is correlation between the temperature dependences of the STE-, LE(AD)-, and Lu_{Al}-AD-luminescence intensities (Fig. 3b) and the corresponding dependences of the intensities of the super-

slow luminescence components for these centers. These results indicate the existence of a metastable level for relaxed state for the above-mentioned centers with a decay time in range 10^{-5}–10^{-3} s.

It should be noted that the decay time constants τ_2 and τ_3, obtained by approximating the decay curves obtained upon synchrotron radiation excitation, are on the whole in agreement with the values of τ_1 and τ_3 for

the LE(AD)- and Lu_{Al}-AD-luminescence components, obtained from the data on the X-ray luminescence kinetics of LuAG single crystals at wavelengths of 280 and 320 nm (Table 1). At the same time, a significant difference of the luminescence decay kinetics of LE(AD) and Lu_{Al}-AD centers upon synchrotron radiation excitation in the exciton region (Fig. 7a, *1*) from the X-ray luminescence decay kinetics at 77 K (Fig. 8) is in the possibility of detecting very fast (2.1–2.45 ns) components, corresponding to the σ components of the LE(AD) and Lu_{Al} luminescence, whereas X-ray excitation allows one to study more thoroughly the π luminescence components of these centers.

The luminescence decay kinetics of Pb^{2+} ions in the UV band (curve *1*) and in the visible range (curve *2*) in single-crystal LuAG films is shown in Fig. 6b. For comparison, Fig. 6b shows also the shape of the synchrotron radiation excitation pulse (curve *3*). The data in Fig. 6b indicate that the decay kinetics of the UV luminescence band of Pb^{2+} ions is much faster than the luminescence decay kinetics in the visible range, which is evidence of the different nature of luminescence excitation for these centers in single-crystal films. In particular, the luminescence decay curves in the UV and visible spectral ranges can be approximated by a set of three exponentials with the decay time constants $\tau_1 = 0.81$ ns, $\tau_2 = 25.6$ ns, and $\tau_3 = 420$ ns (UV range) and $\tau_1 = 0.81$ ns, $\tau_2 = 80.7$ ns, and $\tau_3 = 9$ μs (visible range). Since the duration of the fast luminescence components (0.81 ns) is comparable with the width of the synchrotron radiation pulse, we do not draw here any particular conclusions about the nature of these components. The presence of two other component, fast (τ_2) and slow (τ_3), with the decay time constants lying, respectively, in the nanosecond and microsecond ranges, is typical of the luminescence of ns^2 ions in oxides [18, 19, 29]. This decay kinetics is indicative of radiative relaxation from two excited levels ($^3P_1$ and $^3P_0$) of the relaxed electronic states of single and pair luminescence centers, formed by Pb^{2+} ions, in the UV and visible spectral regions.

CONCLUSIONS

The intrinsic luminescence in single-crystal LuAG films is determined only by the emission of STEs (4.95 eV) in regular (unperturbed by the presence of ADs) garnet lattice sites, whereas in LuAG single crystals, which are characterized by high (to 0.5 at %) concentrations of Lu_{Al} ADs, radiative exciton relaxation occurs predominantly at the sites of AD localization. In this context, the emission of LE(AD) (4.36 eV) and Lu_{Al}-AD (3.76 eV) centers is dominant in the intrinsic luminescence spectra of LuAG single crystals.

The positions of the STE luminescence excitation maxima for single-crystal LuAG films (7.4 and 7.71 eV) differs significantly from the positions of the corresponding maxima for LE(AD) (7.06 and 7.45 eV)

and Lu_{Al}-AD (7.01 and 7.46 eV) centers in LuAG single crystals. Note another important feature of the STE luminescence in single-crystal LuAG films, where the intensity of this luminescence under excitation in the region of interband transitions (Fig. 2a, curve *2*) is much lower (by an order of magnitude) in comparison with the excitation intensity in the exciton region (Fig. 2a, curves *1*, *4*). The low STE luminescence intensity of single-crystal LuAG films under interband excitation indicates a small cross section *S* for *e*/*h* recombination of the STE components at regular garnet lattice sites [24]. At the same time, the cross section *S* significantly increases when impurities or defects are present; specifically this situation is implemented in LuAG single crystals with high (up to 0.5 at %) concentrations of Lu_{Al} ADs.

The relatively small Stokes shift (2.45 eV) and low STE luminescence intensity in single-crystal LuAG films, especially upon excitation in the region of interband transitions (Fig. 2a, curve *2*), indicate that the structure of STEs in this garnet significantly differs from that in alkali halide crystals, which are characterized by high STE luminescence intensity upon interband excitation [30]. This effect is due to the large values of *S* at two-halide self-trapping of holes. Therefore, in contrast to alkali halide crystals, we can suggest that, as in the case of simple oxides Al_2O_3 and Y_2O_3 [23–26], the STE luminescence in LuAG is due to radiative relaxation of the excitons formed by electrons localized at $6s + 5d$ levels of Lu^{3+} cations with self-trapped holes formed by nonbonding $2p$ orbitals of singly charged O^- ions.

We should also note that doping of single-crystal films and single crystals of this garnet with Ce^{3+} ions leads to a significant change in the spectral kinetic characteristics of exciton luminescence. Specifically, the luminescence of LE(AD) and LE(Pb) centers in undoped single crystals and single-crystal LuAG films plays a key role, whereas the STE luminescence dominates in the UV range in the luminescence and luminescence excitation spectra of LuAG:Ce single crystals and single-crystal films (Fig. 2a, curve *4* and Fig. 7, curve *1*; see also [2, 3]). This conclusion is somewhat unexpected is we do not take into account the efficient energy transfer between LE(AD) and Lu_{Al}^{3+}-AD centers and Ce^{3+} ions in LuAG:Ce single crystals, as well as between LE(Pb) and Pb^{2+} centers and Ce^{3+} ions in single-crystal LuAG:Ce films. A detailed investigation of the conditions for this excitation energy transfer between Lu_{Al} ADs and Ce^{3+} ions in LuAC:Ce single crystals was performed by us previously [2, 3]. The results of similar investigations of the excitation energy transfer from LE(Pb) centers and Pb^{2+} ions to Ce^{3+} ions in single-crystal LuAG films were reported in [29].

The result of such excitation energy transfer is that, upon excitation in the exciton region, STE luminescence is dominant in the UV spectral range in the luminescence spectra of LuAG:Ce single crystals and sin-

gle-crystal films, in contrast to the spectra of LuAG single crystals and single-crystal films, where the luminescence of LE(AD) and LE(Pb) centers domains at high concentrations of these defects and impurities.

The parameters of the energy structure of STE, LE(AD), and Lu_{Al}-AD centers in LuAG single crystals and STE, LE(Pb), and Pb^{2+} centers in LuAG and LuAG:Ce single-crystal films are generalized in Table 2. The differences in the spectral kinetic characteristics of the intrinsic luminescence of LuAG and LuAG:Ce single crystals and single-crystal films [2, 3], listed in Table 2, are due to significantly different concentrations of defects of prevailing type or impurities (Lu_{Al} ADs in single crystals and Pb^{2+} ions in single-crystal films). The high (~0.5 at %) AD concentration in LuAG and LuAG:Ce single crystals is determined by the conditions of their high-temperature crystallization from melt by the Czochralski method. In contrast, in the case of LuAG and LuAG:Ce single-crystal films, grown by LPE, it is possible to significantly decrease the concentration K_s of Pb^{2+} ions in the composition of single-crystal films by changing their growth temperature. As a result, one can obtain phosphors based on single-crystal LuAG:Ce films with better spectral kinetic characteristics in comparison with the corresponding single crystals. In particular, single-crystal films of these phosphors are characterized by much faster decay kinetics and smaller contribution of slow luminescence components to the total specific light yield of scintillations [2–4, 31], because these phosphors do not contain luminescence centers and trapping centers formed by Lu_{Al} ADs [32, 33].

REFERENCES

1. Y. Zorenko, A. Voloshinovskii, I. Konstankevych, et al., Radiat. Meas. **38**, 677 (2004).

2. Yu. Zorenko, V. Gorbenko, A. Voloshinovskii, et al., Phys. Status Solidi A **202** (6), 1113 (2005).

3. Yu. V. Zorenko, V. I. Gorbenko, G. B. Stryganyuk, et al., Opt. Spektrosk. **99** (6), 957 (2005) [Opt. Spectrosc. **99**, 923 (2005).

4. Yu. Zorenko, V. Gorbenko, I. Konstankevych, et al., J. Lumin. **114** (4), 85 (2005).

5. Yu. V. Zorenko, I. V. Onstankevich, V. V. Mikhaĭlin, et al., Opt. Spectrosc. **96**, 390 (2004).

6. M. Kirm, A. Lushchik, Ch. Lushchik, and G. Zimmerer, ECS Proceeding Volume **99–40**, 113 (1999).

7. A. I. Kuznetsov, B. R. Namozov, and V. V. Murk, Phys. Solid State **27**, 3030 (1985).

8. V. Murk and N. Jaroshevich, J. Phys.: Condens. Matter **7**, 5857 (1995).

9. M. Nikl, J. Maresh, N. Solovieva, et al., Phys. Status Solidi A **201**, R41 (2004).

10. M. Kh. Ashurov, Yu. K. Voronko, V. V. Osiko, and A. A. Sobol, Phys. Status Solidi A **42**, 101 (1977).

11. S. Geller, J. P. Espinosa, L. D. Fullmer, and P. B. Grandall, Mater. Res. Bull. **7**, 1219 (1972).

12. Yu. Zorenko, I. Konstankevych, V. Gordenko, and P. Yurchyshyn, J. Appl. Spectrosc. **69** (5), 665 (2002).

13. Yu. Zorenko, V. Gorbenko, I. Konstankevych, et al., Nucl. Instrum. Methods Phys. Res., Sect. A **486**, 309 (2002).

14. G. B. Scott and J. L. Page, J. Appl. Phys. **48**, 1342 (1977).

15. V. Babin, K. Blazek, A. Krasnikov, et al., Phys. Status Solidi C **2**, 97 (2005).

16. M. Springis, A. Pujats, and J. Valbis, J. Phys.: Condens. Matter **3**, 5457 (1991).

17. A. Pujats and M. Springis, Radiat. Eff. Defects Solids **155**, 65 (2001).

18. Yu. Zorenko, T. Voznyak, V. Gorbenko, et al., HASYLAB Annual Report (2005), p. 423.

19. V. Babin, V. Gorbenko, A. Makhov, et al., Phys. Status Solidi C **4** (3), 797 (2007).

20. Yu. Zorenko, V. Gorbenko, T. Voznyak, et al., Radiat. Meas. **42** (4–5), 882 (2007).doi:10.1016/j.radmeas.2007.02.030.

21. V. Nagirnyi, S. Zazubovych, S. Zepelin, et al., Chem. Phys. Lett. **227**, 533 (1994).

22. Sh. Tanimizu, *Phosphors Handbook,* Ed. by Sh. Shinoya and W. M. Yen (CRC Press LLC, New York, 2000), p. 141.

23. A. Lushchik, M. Kirm, E. Feldbach, et al., J. Lumin. **87–89**, 232 (2000).

24. B. R. Namozov, M. E. Fominich, V. V. Murk, and R. I. Zaharchenya, Phys. Solid State **40** (5), 910 (1998).

25. M. Kirm, G. Zimmerer, E. Feldbach, et al., Phys. Rev. **60**, 502 (1999).

26. A. Lushchik, E. Feldbach, M. Kirm, et al., Relat. Phenom. **101–103**, 587 (1999).

27. Yu. Zorenko, V. Gorbenko, A. Voloshinovskii, G. Stryganyuk, S. Nelidko, V. Degoda, O. Chukova, Phys. Stat. Sol. C **2** (1), 105–108 (2005.)

28. Yu. V. Zorenko, Opt. Spektrosk. **100** (4), 617 (2006) [Opt. Spectrosc. **100**, 572 (2006)].

29. V. Babin, A. Makhov, M. Nikl, et al. J. Lumin. **127** (2), 384 (2007).

30. Ch. Lushchik, A. Lushchik, T. Karner, et al., Russ. Phys. J. **43**, 171 (2002).

31. Yu. Zorenko, V. Gorbenko, I. Konstankevych, et al., in *Proc. SCINT, Alushta, Ukraine, 2005* (Kharkiv, 2006), p. 428.

32. M. Nikl, E. Mihokova, J. Pejchal, et al., Phys. Status Solidi B **242**, R119 (2005).

33. A. Vedda, M. Fasoli, F. Moretti, et al., in *Proc. SCINT, Alushta, Ukraine, 2005* (Kharkiv, 2006), p. 235.

Translated by Yu. Sin'kov